



# Thermoconvection in magnetized ferrofluids: the influence of boundaries with finite heat conductivity

A. Recktenwald, M. Lücke\*

*Institut für Theoretische Physik, Universität des Saarlandes, D-66041 Saarbrücken, Germany*

Received 13 January 1998

---

## Abstract

Realistic boundaries of finite heat conductivity for thermoconvection in a Rayleigh–Bénard setup with magnetized ferrofluids are investigated. A linear stability analysis of the conductive state is performed with a shooting method. It shows that the critical wave number is for any magnetic field strongly influenced by the conductivity of the boundaries. Linear as well as nonlinear coefficients of a Ginzburg–Landau amplitude equation for convection shortly above the onset are evaluated as functions of the magnetic Rayleigh number, the boundary conductivities, and the fluid Prandtl number. © 1998 Elsevier Science B.V. All rights reserved.

*PACS:* 83.80.Gv; 47.20.Bp; 47.20.Ky; 47.65. + a

*Keywords:* Magnetic fluids; Buoyancy-driven instability; Nonlinearity; Magnetohydrodynamics

---

## 1. Introduction

Convection of magnetic fluids in the classical Rayleigh–Bénard setup in the presence of a vertical magnetic field has been studied theoretically by Finlayson [1]. However, the experiments by Schwab et al. [2,3] showed that the theoretical critical wave numbers of the flow structure were larger than those that were measured in the experiments carried out with horizontal plates of finite heat conductivity. In this paper we investigate how, with decreasing conductivity of the plates, linear

and weakly nonlinear convection properties change.

We consider a horizontal fluid layer of height  $d$  between horizontal plates each of thickness  $d_p$  subjected to a homogeneous vertical ( $z$ -direction) gravitational acceleration  $g$  and a homogeneous vertical magnetic field. The ratio of the thermal conductivities of the plates,  $A_p$ , and of the fluid,  $A_f$ , is  $\zeta = A_p/A_f$  and  $\delta = d_p/(d/2)$  is the plate thickness in units of half the height of the fluid layer. Then the vertical temperature profile in the conductive, quiescent state without convection is piecewise linear as shown in Fig. 1 for the case of  $\delta = 1$ . A temperature difference  $\Delta T$  imposed between the outer surfaces of the plates at  $z = \pm (d/2 + d_p)$  implies

---

\* Corresponding author. E-mail: luecke@lusi.uni-sb.de.

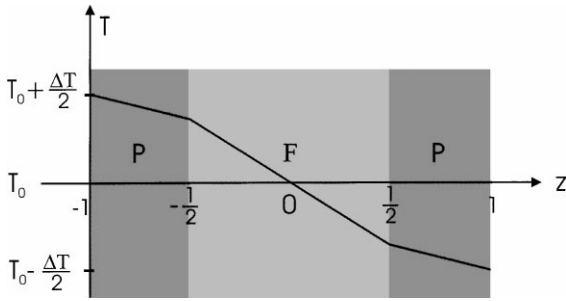


Fig. 1. Vertical temperature profile of the quiescent conductive state in the plates (P) and in the fluid (F) here shown for  $\delta = d_p/(d/2) = 1$ . With  $\Delta T$  being imposed externally the conductive temperature difference across the fluid layer is  $\Delta T_F = \Delta T/(1 + \delta/\zeta)$ .

a temperature difference

$$\Delta T_F = \frac{\Delta T}{1 + \delta/\zeta} \quad (1.1)$$

across the fluid layer in the conductive state. We use this conductive  $\Delta T_F$  to define the Rayleigh number

$$Ra = \frac{\alpha g d^3 \Delta T_F}{\kappa \nu} \quad (1.2)$$

and the magnetic Rayleigh number

$$N = \frac{\mu_0 K^2 d^2 (\Delta T_F)^2}{\kappa \eta (1 + \chi)} \quad (1.3)$$

as control parameters. A negative value of  $\Delta T$  or of  $\Delta T_F$  stands for heating of the upper plate and a positive one for lower plate heating. Here  $\alpha$  is the thermal expansion coefficient,  $\kappa$  the thermal diffusivity,  $\nu$  the kinematic viscosity, and  $\eta$  the effective viscosity of the fluid. Furthermore,  $\mu_0$  is the magnetic field constant,  $\chi$  the magnetic susceptibility, and  $K$  is the pyromagnetic coefficient, which is almost proportional to the external magnetic field.

For convenience,  $Ra$  and  $N$  are normalized by the critical Rayleigh number  $Ra_c^0$  for onset of convection in a fluid bounded by plates of conductivity  $A_p$  and thickness  $d_p$  in the absence of a magnetic field. So we introduce

$$r = \frac{Ra}{Ra_c^0}, \quad n = \frac{N}{3Ra_c^0}. \quad (1.4)$$

## 2. Equations and boundary conditions

Henceforth we scale positions by the height of the fluid layer  $d$ , time by  $d^2/\kappa$ , velocity by  $\kappa/d$ , temperature by  $\Delta T_F$ , and the vertical magnetic field by  $d^2 K \beta / (1 + \chi)$ . Using this scaling we get from the basic hydrodynamic field equations [1] the following system of partial differential equations:

$$\begin{aligned} \frac{1}{\sigma} \partial_t \nabla^2 w &= \nabla^4 w + (\partial_x^2 + \partial_y^2)[(Ra + N)\theta - N\varphi] \\ &- \frac{1}{\sigma} \nabla \times \nabla \times [(\mathbf{v} \cdot \nabla) \mathbf{v}]_z + N[\partial_y(\partial_y \theta \partial_z \varphi \\ &- \partial_z \theta \partial_y \varphi) + \partial_x(\partial_x \theta \partial_z \varphi - \partial_z \theta \partial_x \varphi)], \end{aligned} \quad (2.1a)$$

$$\partial_t \theta = \nabla^2 \theta + w - (\mathbf{v} \cdot \nabla) \theta, \quad (2.1b)$$

$$\nabla^2 \varphi = \partial_z^2 \theta, \quad (2.1c)$$

for the deviations from the quiescent state of heat conduction in the fluid. Here  $w = \mathbf{v} \cdot \mathbf{e}_z$  is the vertical velocity field,  $\theta = T - T_{\text{cond}}$ ,  $\varphi = (\mathbf{H} - \mathbf{H}_{\text{cond}}) \cdot \mathbf{e}_z$ , and  $\sigma = \nu/\kappa$  is the Prandtl number. The pressure was eliminated by applying twice the rotation to the momentum balance equation.

The equations are solved subject to the following realistic boundary conditions: the plates are rigid, thus enforcing the no-slip condition

$$w = \partial_z w = 0 \quad \text{at } z = \pm \frac{1}{2} \quad (2.2a)$$

on the velocity field. The boundary conditions on the deviations of the temperature in the plates,  $\tilde{\theta}$ , and in the fluid,  $\theta$ , from the conductive profile of Fig. 1 are

$$\partial_z \theta = \zeta \partial_z \tilde{\theta}, \quad \theta = \tilde{\theta} \text{ at } z = \pm \frac{1}{2} \quad (2.2b)$$

to ensure continuity of the heat flux and of the temperature. With  $\Delta T$  being imposed externally one has

$$\tilde{\theta} = 0 \quad \text{at } z = \pm \frac{1}{2}(1 + \delta). \quad (2.2c)$$

The vertical magnetic field deviation from the magnetic field in the conductive state,  $\varphi = (\mathbf{H} - \mathbf{H}_{\text{cond}}) \cdot \mathbf{e}_z$ , has to fulfill the condition

$$(1 + \chi) \partial_z \varphi \pm k \varphi = 0 \quad \text{at } z = \pm \frac{1}{2}. \quad (2.2d)$$

Here  $k$  is the wave number of the convective roll structure that bifurcates out of the conductive state.

### 3. Linear analysis

We have performed a standard linear stability analysis of the conductive state for plane wave perturbation fields obeying the above boundary conditions (2.2). To that end the linearized version of the field equations of the ferrofluid (Eqs. (2.1a), (2.1b) and (2.1c)) coupled to the heat diffusion equation in the plates were solved by a shooting method [4]. The resulting critical eigenfunctions are plotted in Fig. 2 for different magnetic fields at  $\delta = 1$  and  $\zeta = 5$ . The latter being the conductivity ratio realized in the experimental setup of Schwab et al. [2,3]. The maximal amplitude of the vertical velocity  $\hat{w}(z)$  increases with growing magnetic field, i.e., with growing  $n$  while that of the lateral velocity  $\hat{u}(z)$ , of the temperature  $\hat{\theta}(z)$ , and of the magnetic field  $\hat{\phi}(z)$  is decreasing with increasing  $n$  without much change in the profiles. The discontinuous slope of  $\hat{\theta}(z)$  at  $z = \pm \frac{1}{2}$  comes from the continuity of the heat flux. Here we used the normalization  $\int dz \hat{w}(z)\hat{\theta}(z) = 1$ .

From the neutral stability problem one finds that the instability is a stationary one as for boundaries with infinite conductivity,  $\zeta = \infty$ . The critical Rayleigh number  $r_c(n)$  and the corresponding critical wave number  $k_c(n)$  as a function of the magnetic Rayleigh number  $n$  are shown in Figs. 3 and 4, respectively, for  $\delta = 1$  and several  $\zeta$ . Both  $k_c$  and  $r_c$  shift to smaller values when the conductivity of the plates decreases. The variation of  $r_c(n)$  with  $n$  can be fitted reasonably well by a linear law. The fitted coefficients are presented in Table 1 for several values of  $\zeta$ .

The symbols in Figs. 3 and 4 refer to Rayleigh numbers and wave numbers that were observed at the onset of convection in experiments carried out with fluid layers of different heights  $d$  between 1 and 4 mm and an upper plate of fixed thickness  $d_p = 6$  mm with reduced conductivity  $\zeta = 5$  [3]. Our linear analysis showed for such values of  $\delta \geq 3$  that  $r_c$  and  $k_c$  had well reached their large- $\delta$  asymptotic plateau behavior: both  $r_c$  and  $k_c$  decrease in the range  $0 < \delta < 1$  with growing  $\delta$  and have ap-

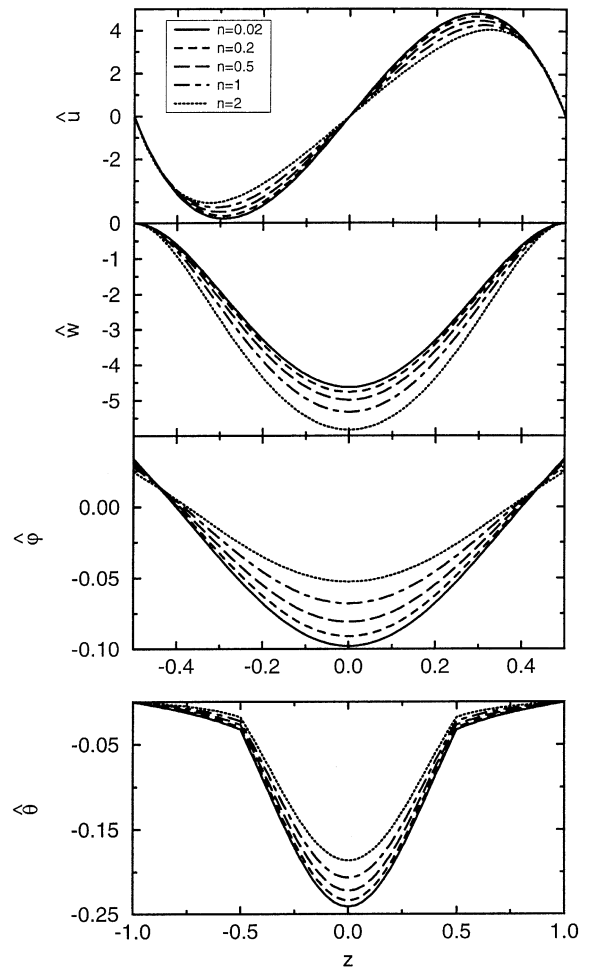


Fig. 2. Vertical variation of the linear critical eigenfunctions of lateral velocity  $\hat{u}$ , vertical velocity  $\hat{w}$ , magnetic field  $\hat{\phi}$ , and temperature  $\hat{\theta}$  for  $\zeta = 5$ ,  $\delta = 1$ , and different reduced magnetic Rayleigh numbers  $n$ .

proached their large- $\delta$  constant asymptote around  $\delta = 1$  so that at  $\delta > 1$  there is no more significant variation with  $\delta$ . Note in addition that the influence of  $\delta$  on convection properties decreases with growing conductivity  $\zeta$  of the plate – the thermal stress on the fluid,  $\Delta T_F$ , which determines the driving (1.2) and (1.3) approaches  $\Delta T$  for  $\zeta \rightarrow \infty$  and the fluid approaches the limiting situation of being bound by perfectly heat conducting plates.

Our results agree in the nonmagnetic limit,  $n = 0$ , with the linear stability analysis of Jenkins

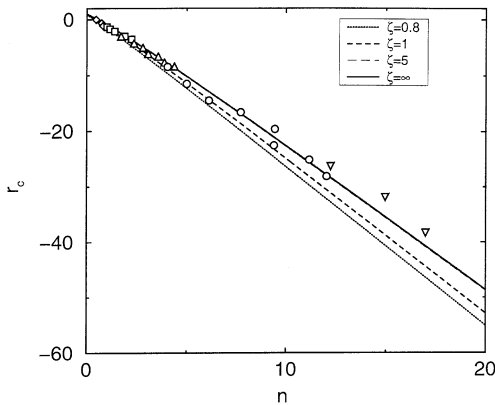


Fig. 3. Critical Rayleigh number  $r_c$  versus magnetic Rayleigh number  $n$  for different  $\zeta$  and  $\delta = 1$ ,  $\chi = 1$ . The curves for  $\zeta = 5$  and  $\zeta = \infty$  are practically identical. Symbols refer to experimentally observed convective thresholds [3] in setups with  $\zeta = 5$  and  $\delta = 3$  ( $\nabla$ ), 4 ( $\circ$ ), 6 ( $\triangle$ ), 8 ( $\square$ ), and 12 ( $\diamond$ ). See text for further discussion.

et al. [5] for all  $\zeta$ . Furthermore, in the presence of a magnetic field we confirm the theoretical results of Schwab [3] and Stiles et al. [6] reported for the limit  $\zeta = \infty$ . We have no explanation for the fact that the wave numbers (symbols in Fig. 4) that were observed to be selected by convective patterns close to onset in the experimental setup of Schwab et al. [3] lie closer to the  $\zeta = 1$  theoretical critical wave numbers than to the  $\zeta = 5$  curve.

#### 4. Weakly nonlinear analysis

Slightly above the stability threshold the nonlinear convective state can be approximately described by

$$\mathbf{Y}(x, z, t) = (u, w, \theta, \varphi)^T = A(x, t)\hat{\mathbf{Y}}(z)e^{ik_c x} + \text{c.c.} \quad (4.1)$$

Here  $\hat{\mathbf{Y}}(z)$  is the eigenvector of the linear problem at the critical point presented in Fig. 2 and  $A(x, t)$  is the saturation amplitude of the critical mode determined by the nonlinearity in the field equations. For slightly supercritical driving ( $0 \leq \varepsilon = r - r_c \ll 1$ ) a small band of lateral wave numbers with  $|k - k_c| = \mathcal{O}(\varepsilon^{1/2})$  is excited, giving rise to a slow spatiotemporal variation of the convective roll structure. These slow variations of the amplitude  $A$  are conveniently captured by the method of mul-

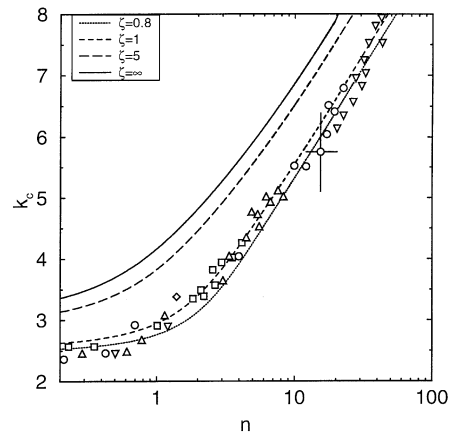


Fig. 4. Critical wave number  $k_c$  versus magnetic Rayleigh number  $n$  for different  $\zeta$  and  $\chi = 1$ . Symbols refer to experimentally observed wave numbers of convection patterns close to threshold [3] in setups with  $\zeta = 5$  and different  $\delta$  identified in Fig. 3. See text for further discussion.

tiples scales [7]. It enables the Ginzburg–Landau amplitude equation [8,9] to be derived in a straightforward manner

$$\tau_0 \partial_t A(x, t) = [\varepsilon + \zeta_0^2 \partial_x^2 - \gamma |A(x, t)|^2] A(x, t) \quad (4.2)$$

from the hydrodynamic field equations.

We have determined the coefficients  $\tau_0$ ,  $\zeta_0^2$ , and  $\gamma$  of this equation for rigid boundaries with different  $\zeta$  by numerically evaluating special scalar products of the eigenfunctions [10]. Since the coefficients with no magnetic field, i.e., for an ordinary fluid, have not yet been presented in the literature as a function of  $\zeta$  we show them in Fig. 5 for  $\delta = 1$ . The linear coefficients  $\tau_0$  and  $\zeta_0^2$  are presented in Fig. 6 as functions of the magnetic Rayleigh number  $n$ . The nonlinear coefficient  $\gamma$  shows a linear dependence on  $n$ , i.e.,

$$\gamma(\zeta, n) = \gamma_0(\zeta) + b_\gamma(\zeta)n. \quad (4.3)$$

The expansion coefficients  $\gamma_0(\zeta)$  and  $b_\gamma(\zeta)$  are given in Table 1 for several  $\zeta$ .

To evaluate the slope  $\partial \text{Nu} / \partial n$  of the Nusselt number at the critical point we start from the relation

$$\text{Nu}(r, n) = 1 + \frac{r - r_c(n)}{\gamma(n)} \quad (4.4)$$

Table 1  
Fitting-coefficients for the  $n$  dependence of  $r_c$ ,  $\gamma$ , and  $\partial\text{Nu}/\partial n|_c$  for different  $\zeta$

$\zeta$	0.8	1	2	5	10	100	1000	$\infty$
$r_c = 1 - b_r n$								
$\text{Ra}_c^0$	1256.9669	1303.4412	1439.8249	1574.0344	1634.8154	1699.8132	1706.9597	1707.7618
$b_r$	2.424	2.403	2.349	2.304	2.283	2.265	2.262	2.259
$\gamma = \gamma_0 + b_\gamma n$								
$\gamma_0$	0.6120	0.6145	0.6330	0.6634	0.6802	0.6991	0.7023	0.7027
$b_\gamma$	1.0709	1.1223	1.2656	1.3883	1.4468	1.4992	1.4594	1.4243
$\partial\text{Nu}/\partial n _c = 1/(a - br_c)$								
$a$	0.434	0.450	0.498	0.549	0.575	0.601	0.596	0.590
$b$	0.182	0.194	0.229	0.262	0.277	0.292	0.285	0.279

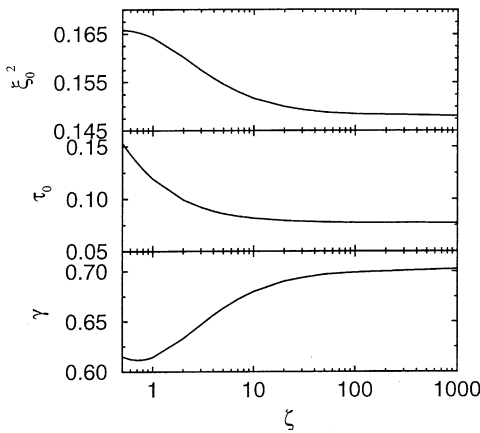


Fig. 5. Coefficients of the amplitude equation as functions of  $\zeta$  without magnetic field,  $n = 0$ . The normalization of the critical eigenfunction entering into  $\gamma$  was chosen to be  $\int dz \hat{w}(z) \hat{\theta}(z) = 1$ .

that holds close to onset,  $r - r_c(n) \ll 1$ . Thus

$$\left. \frac{\partial \text{Nu}}{\partial n} \right|_c = - \frac{1}{\gamma(n)} \frac{\partial r_c(n)}{\partial n}. \quad (4.5)$$

Since  $r_c(n) \simeq 1 - b_r n$  one can rewrite Eq. (4.3) as  $\gamma = \gamma_0 + b_\gamma(1 - r_c)/b_r$  to obtain  $\partial\text{Nu}/\partial n|_c$  in the more compact form

$$\left. \frac{\partial \text{Nu}}{\partial n} \right|_c = \frac{1}{a - br_c}. \quad (4.6)$$

The fit coefficients  $b = b_\gamma/b_r^2$  and  $a = b + (\gamma_0/b_r)$  are presented in Table 1. Graphs for different  $\zeta$  are given in Fig. 7.

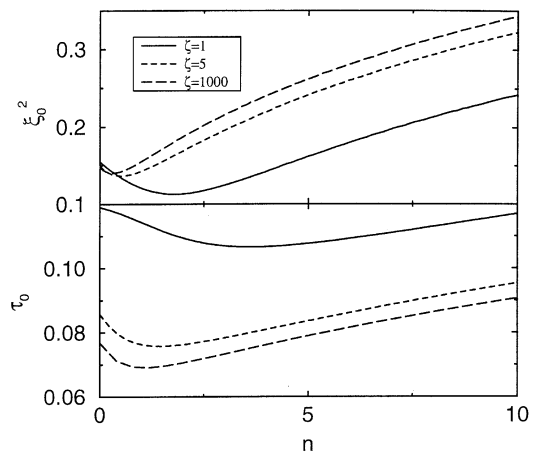


Fig. 6. Linear coefficients  $\tau_0$  and  $\xi_0^2$  of the amplitude equation as functions of the magnetic Rayleigh number  $n$  for different  $\zeta$ . The long-dashed curves for  $\zeta = 1000$  are practically the same as for perfectly heat conducting plates with  $\zeta = \infty$ .

## 5. Prandtl number dependence

The results presented so far refer to fluids of Prandtl number  $\sigma = 1$ . Now we discuss the  $\sigma$  dependence for the case of perfectly heat conducting plates,  $\zeta = \infty$ . The  $\sigma$  dependence for finite  $\zeta$ , say,  $\zeta \gtrsim 1$  is similar. The marginal stability curve and the linear eigenfunctions of the stationary eigenvalue problem have no Prandtl number dependence. Thus  $r_c$ ,  $k_c$ , and  $\xi_0^2$  are  $\sigma$ -independent. However,  $\tau_0$  depends on  $\sigma$ . Graphs for different  $n$  are given in Fig. 8 for  $\zeta = \infty$ . Note that the difference

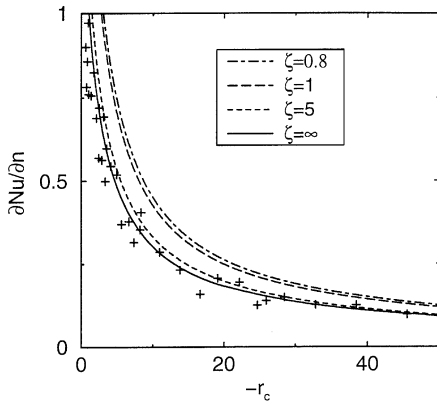


Fig. 7. Initial slope of the Nusselt number versus critical Rayleigh number. Symbols refer to experimental results obtained with plates of large heat conductivity [3].

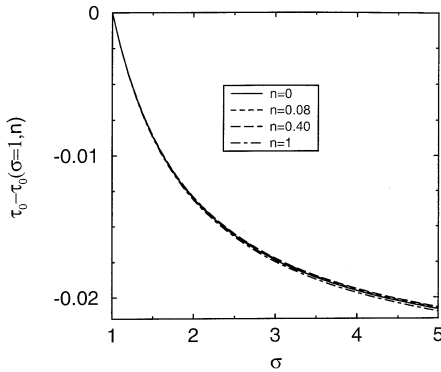


Fig. 8. Linear coefficient  $\tau_0(\sigma, n) - \tau_0(\sigma = 1, n)$  versus  $\sigma$  for different magnetic Rayleigh numbers  $n$ .

$\tau_0(\sigma, n) - \tau_0(\sigma = 1, n)$  is practically independent of  $n$ . This implies that  $\tau_0(\sigma, n)$  can be approximated well by

$$\tau_0(\sigma, n) - \tau_0(\sigma = 1, n) = \frac{\sigma + 0.5117}{19.65\sigma} - 0.0769 \quad (5.1)$$

for  $\zeta = \infty$  and the right-hand side of Eq. (5.1) is just  $\tau_0(\sigma, n = 0)$  [11] for the case without the magnetic field. Thus one only needs to know  $\tau_0(\sigma = 1, n)$ , which can be taken from the long-dashed curve in the lower part of Fig. 8. It represents  $\tau_0(\sigma = 1, n, \zeta = 1000)$ , which is practically the same as  $\tau_0(\sigma = 1, n, \zeta = \infty)$ .

Table 2

Fit coefficients for the  $\sigma$  dependence of  $\gamma(n, \sigma) = \gamma^{(0)}(n) - \gamma^{(1)}(n)/\sigma + \gamma^{(2)}(n)/\sigma^2$  for different  $n$

$n$	$\gamma^{(0)}$	$\gamma^{(2)}$	$\gamma^{(1)}$
0	0.699	0.00832	0.00471
0.01	0.710	0.00966	0.00453
0.04	0.745	0.00941	0.00547
0.08	0.792	0.00916	0.00673
0.16	0.888	0.00864	0.00895
0.2	0.945	0.00851	0.00102
0.4	1.212	0.00728	0.01411
0.8	1.756	0.00568	0.01867
1	2.014	0.00502	0.02035

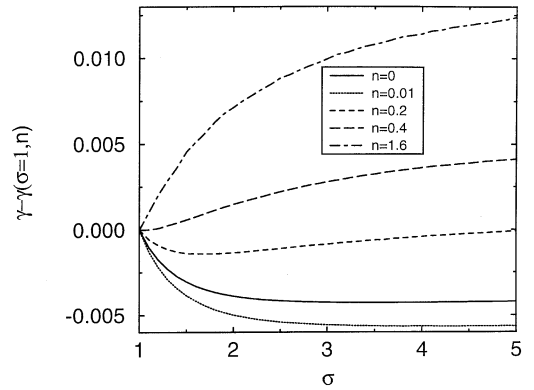


Fig. 9. Nonlinear coefficient  $\gamma(\sigma, n) - \gamma(\sigma = 1, n)$  versus  $\sigma$  for different magnetic Rayleigh numbers  $n$ .

The  $\sigma$  dependence of the nonlinear coefficient  $\gamma$  can be fitted by the expression

$$\gamma(n, \sigma) = \gamma^{(0)}(n) - \frac{\gamma^{(1)}(n)}{\sigma} + \frac{\gamma^{(2)}(n)}{\sigma^2}. \quad (5.2)$$

The fitting coefficients  $\gamma^{(i)}(n)$  are presented in Table 2 for several  $n$ . For  $\sigma = 1$  the  $n$  variation is practically linear, i.e.,  $\gamma(\sigma = 1, n) = 0.7027 + 1.42427n$ . Graphs of the difference  $\gamma(\sigma, n) - \gamma(\sigma = 1, n)$  are given in Fig. 9. For Prandtl number larger than 10 the dependence on  $\sigma$  can be neglected and one can use  $\sigma = \infty$ .

**Acknowledgements**

Support by the Deutsche Forschungsgemeinschaft is gratefully acknowledged.

**References**

- [1] B.A. Finlayson, *J. Fluid Mech.* 40 (1970) 753.
- [2] L. Schwab, U. Hildebrandt, K. Stierstadt, *J. Magn. Magn. Mater.* 39 (1983) 113.
- [3] L. Schwab, Ph.D. thesis, Universität München, 1989.
- [4] J. Stoer, R. Bulirsch, *Einführung in die Numerische Mathematik II*, Springer, Berlin, 1978.
- [5] D.R. Jenkins, M.R.E. Proctor, *J. Fluid Mech.* 139 (1984) 461.
- [6] P.J. Stiles, M. Kagan, *J. Magn. Magn. Mater.* 85 (1990) 196.
- [7] C.M. Bender, S.A. Orszag, *Advanced Mathematical Methodes for Scientists and Engineers*, McGraw-Hill, New York, 1978.
- [8] L.A. Segel, *J. Fluid Mech.* 38 (1969) 203.
- [9] A.C. Newell, J.A. Whitehead, *J. Fluid Mech.* 38 (1969) 279.
- [10] A. Recktenwald, M. Lücke, H.W. Müller, *Phys. Rev. E* 48 (1993) 4444.
- [11] M.C. Cross, P.C. Hohenberg, *Rev. Mod. Phys.* 65 (1993) 962.